

# Effect of Applied Voltage, Initial Concentration, and Natural Organic Matter on Sequential Reduction/Oxidation of Nitrobenzene by Graphite Electrodes

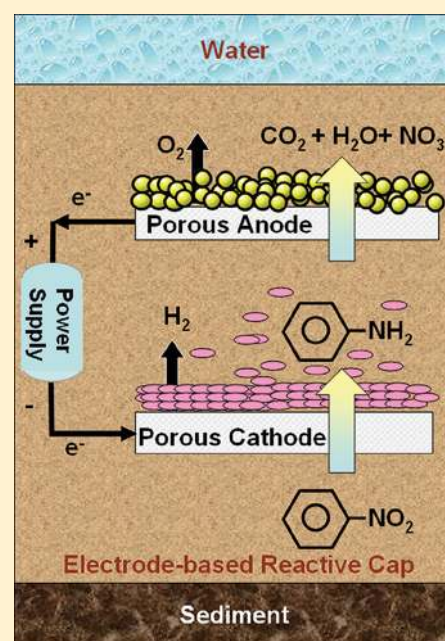
Mei Sun,<sup>†</sup> Danny D. Reible,<sup>§</sup> Gregory V. Lowry,<sup>†,‡</sup> and Kelvin B. Gregory<sup>†,\*</sup>

<sup>†</sup>Department of Civil & Environmental Engineering and <sup>‡</sup>Department of Chemical Engineering Carnegie Mellon University, Pittsburgh, Pennsylvania 15213-3890, United States

<sup>§</sup>Environmental & Water Resources Engineering, University of Texas, Austin, Texas 78712, United States

**S** Supporting Information

**ABSTRACT:** Carbon electrodes are proposed in reactive sediment caps for in situ treatment of contaminants. The electrodes produce reducing conditions and H<sub>2</sub> at the cathode and oxidizing conditions and O<sub>2</sub> at the anode. Emplaced perpendicular to seepage flow, the electrodes provide the opportunity for sequential reduction and oxidation of contaminants. The objectives of this study are to demonstrate degradation of nitrobenzene (NB) as a probe compound for sequential electrochemical reduction and oxidation, and to determine the effect of applied voltage, initial concentration, and natural organic matter on the degradation rate. In H-cell reactors with graphite electrodes and buffer solution, NB was reduced stoichiometrically to aniline (AN) at the cathode with nitrosobenzene (NSB) as the intermediate. AN was then removed at the anode, faster than the reduction step. No common AN oxidation intermediate was detected in the system. Both the first order reduction rate constants of NB ( $k_{\text{NB}}$ ) and NSB ( $k_{\text{NSB}}$ ) increased with applied voltage between 2 V and 3.5 V (when the initial NB concentration was 100  $\mu\text{M}$ ,  $k_{\text{NB}} = 0.3 \text{ h}^{-1}$  and  $k_{\text{NSB}} = 0.04 \text{ h}^{-1}$  at 2 V;  $k_{\text{NB}} = 1.6 \text{ h}^{-1}$  and  $k_{\text{NSB}} = 0.64 \text{ h}^{-1}$  at 3.5 V) but stopped increasing beyond the threshold of 3.5 V. When initial NB concentration decreased from 100 to 5  $\mu\text{M}$ ,  $k_{\text{NB}}$  and  $k_{\text{NSB}}$  became 9 and 5 times faster, respectively, suggesting that competition for active sites on the electrode surface is an important factor in NB degradation. Presence of natural organic matter (in forms of either humic acid or Anacostia River sediment porewater) decreased  $k_{\text{NB}}$  while slightly increased  $k_{\text{NSB}}$ , but only to a limited extent ( $\sim$ factor of 3) for dissolved organic carbon content up to 100 mg/L. These findings suggest that electrode-based reactive sediment capping via sequential reduction/oxidation is a potentially robust and tunable technology for in situ contaminants degradation.



## INTRODUCTION

In situ capping is used to contain contaminated sediments by placing a layer of clean sand or sorbent-amended sand at the sediment-water interface as a barrier for contaminant diffusion to the overlying water column.<sup>1–3</sup> Reactive sediment capping employs materials that can transform or degrade contaminants within the cap, thereby better preventing their breakthrough from the cap.<sup>4,5</sup> However, very few, if any, cost-effective materials are available to degrade contaminants within a sediment cap over the long time scales (perhaps decades to centuries) required for in situ sediment remediation.

A recent study<sup>6</sup> evaluated polarized carbon electrodes as reactive capping material for engineering desirable redox gradients as well as the delivery of electron donor for contaminant degradation. A conceptual model of such system is shown in Supporting Information (SI) Figure S1. Briefly, thin layers of carbon electrodes are placed in the sand cap above the

sediment, perpendicular to the direction of seepage flow; contaminants migrating into the cap will be exposed to a reducing environment in the vicinity of the cathode, followed by an oxidizing environment in the vicinity of the anode (the opposite order can also be created by reversing the polarity of the electrodes). Contaminant degradation may occur as a result of microbial activities near each electrode, or due to abiotic reactions at the electrode surfaces. This current study is focused on the use of such a system to degrade contaminants via abiotic redox reactions at the electrodes.

The design of an electrode-based reactive cap for seepage flow conditions requires an understanding of the reaction rates

Received: January 18, 2012

Revised: April 2, 2012

Accepted: May 9, 2012

Published: May 9, 2012

and the impacts of porewater chemistry at the electrode surface. Degradation must be faster than convection through the cap to prevent breakthrough; meanwhile, the reaction rate must also be achievable at reasonably low voltage to minimize energy consumption, as well as pH changes expected from the accumulation of  $H^+_{(aq)}$  and  $OH^-_{(aq)}$  at the anode and cathode, respectively.<sup>6</sup> The effect of cathode potential on reaction rate, selectivity and efficiency in similar electrochemical devices has been studied,<sup>7</sup> but from a practical point of view, applied voltage is more likely to be the controlling parameter in cap design and operation. The applied voltage between the anode and the cathode controls the redox gradient in sediment cap and the evolution rates of electron donor and acceptor,<sup>6</sup> but little is known about the voltage effect on contaminant degradation rates on inexpensive carbon electrodes surfaces.

Another open question about the performance of the electrode-based reactive cap is whether initial contaminant concentration will influence the reaction rate constants. A decrease of the 2,4-dichlorophenoxyacetic acid (2,4-D) dechlorination rate was reported with increasing substrate concentration using Pd loaded carbon felt cathodes.<sup>8</sup> Similar phenomena also occur in other heterogeneous catalytic reactions, such as contaminants degradation on Fe(0) particles surface,<sup>9</sup> as a result of the competitive adsorption onto reactive surface sites between the parent and daughter compounds (and also among the parent compound molecules). In real sediments, contaminant concentrations vary by orders of magnitude between the source zone and the downstream plume. The effect of contaminant concentration on reactivity must be determined for site specific feasibility, cap design and operating conditions, and performance.

In sediment systems, natural organic matter (NOM) is likely to affect contaminant degradation rates, but this influence has not been examined in electrochemical systems. NOM interacts with environmental contaminants in several ways including electron shuttling,<sup>10</sup> covalent binding,<sup>11</sup> competitive sorption,<sup>12</sup> and solubilization.<sup>13</sup> Carbon electrodes should have high affinity for NOM,<sup>14</sup> with the implication that it will adversely affect electrode performance by competitive adsorption. However, interactions such as electron shuttling may increase reactivity.<sup>10</sup>

Certain sediment contaminants require sequential reduction/oxidation for complete mineralization, including nitroaromatics, polychlorinated biphenyls (PCBs), and chlorinated hydrocarbons. Sequential electrochemical reduction/oxidation of perchloroethene (PCE) has been demonstrated in groundwater.<sup>15</sup> The target compound for this study is nitrobenzene (NB), another representative of such contaminants. Nitrobenzene oxidation is difficult even under aerobic condition.<sup>16,17</sup> and may lead to toxic dead-end products.<sup>18</sup> In contrast, reduction of nitrobenzene to aniline easily occurs under anaerobic conditions, and aniline can readily undergo oxidative ring cleavage and mineralization to ammonium and  $CO_2$ .<sup>19,20</sup> in an aerobic environment. Chemical and microbial reduction of nitrobenzene to aniline in a reactive sediment cap containing Fe(0), sorbent, and bacteria has been reported.<sup>5</sup> Nitrobenzene reduction to aniline also occurs in bioelectrochemical systems coupled with acetate oxidation.<sup>21</sup> Complete degradation of nitrobenzene and other nitroaromatics like RDX (hexahydro-1,3,5-trinitro-1,3,5-triazine) and TNT (2,4,6-trinitrotoluene) in a sequential anaerobic/aerobic microbial wastewater treatment process<sup>22</sup> or by sequential oxidation/reduction using  $IrO_2/$

$TaO_5$  doped titanium electrodes<sup>23,24</sup> have been reported. However, the different role of each stage was not identified.

The objectives of this study are to demonstrate the sequential reduction/oxidation of nitrobenzene using polarized graphite electrodes and determine the effect of applied voltage, initial contaminant concentration, and NOM on the degradation rate constants. Data from this study will enable better design of reactive sediment caps,<sup>6</sup> electrode-based remedial approaches,<sup>25</sup> and energy generation from environmentally deployed electrodes.<sup>26–28</sup>

## ■ MATERIALS AND METHODS

**Chemicals.** Nitrobenzene ( $\geq 99.5\%$ ), nitrosobenzene (97%), and aniline (99.9%) were supplied by Sigma-Aldrich (St. Louis, MO). Sodium hydroxide (NaOH), sodium phosphate monobasic ( $NaH_2PO_4$ ), and sodium bicarbonate ( $NaHCO_3$ ) were supplied by Fisher Scientific (Pittsburgh, PA). Humic acid sodium salt (50–60% as humic acid) was purchased from Acros Organics (Morris Plains, NJ).

**Nitrobenzene Degradation Reaction.** Experiments to study nitrobenzene degradation kinetics were carried out at room temperature ( $23 \pm 2$  °C) in two-chamber glass H-cell reactors (SI Figure S2) as described previously.<sup>6</sup> Each chamber contained 60 mL headspace and 250 mL buffer solution, and was well mixed using a magnetic stir bar. Unless stated otherwise, the buffer solution contained 20 mM  $NaH_2PO_4$  adjusted to pH 6.5 by 5% NaOH solution. Such buffer concentration was used in order to match the buffer intensity of Anacostia River (Washington, DC) sediment porewater. Graphite felt (10 cm long  $\times$  4 cm wide  $\times$   $1/4$  in. thick, Wale Apparatus Co., Inc., Hellertown, PA) was used as electrodes. Constant voltage was applied using E3620A DC power supplies (Agilent Technologies, Santa Clara, CA). In each reactor, one chamber had NB together with buffer and is defined as the working chamber, while the other contains buffer only. The electrode in working chamber was connected to the negative pole of a power supply to serve as cathode during reduction and then switched to the positive pole to serve as anode during oxidation. Real-time electrode potential for the working chamber was measured vs Ag/AgCl reference electrodes (Electrolytica, Inc., Amherst, NY), and logged using a model 2700 digital multimeter (Keithley Instruments, Inc., Cleveland, Ohio). Electrode potential is reported as vs standard hydrogen electrode (SHE). After the voltage was applied and electrode potential in working chamber became stabilized, 10 mL of NB stock solution (2.5 mM) was added to achieve an initial NB concentration of  $\sim 100$   $\mu$ M, except in the experiments for initial concentration impact, where the concentration of NB was varied.

**Sediment Porewater Simulation.** In the NOM effect study, the working chamber of the H-cell reactors were filled with simulated sediment porewater with 20 mM  $NaH_2PO_4$  or humic acid solution with 20 mM  $NaH_2PO_4$  (both at pH 6.5), instead of pure buffer solution. Simulated sediment porewater was generated by a modified version of the standard method ASTM D3987. In brief, Anacostia River sediment (moisture content  $46.4 \pm 1.7$  wt %) was mixed with DI water (1:5 sediment: water weight ratio) in a glass bottle and rotated at 30 rpm for 46 h. The mixture was then centrifuged at 2000g for 10 min and filtered with a nominal 20–25  $\mu$ m filter (Whatman, Piscataway, NJ). The dissolved organic carbon (DOC) content of stimulated porewater was 14.4 mg/L as carbon, reasonably close to actual porewater (24 mg/L). Humic acid (HA) sodium

salt was also used as a representative NOM for assessing its impact on reaction rate constants at different concentration.

**Analytical Methods.** Aqueous concentrations of NB, NSB, and AN were quantified by high performance liquid chromatography (HPLC) (Agilent, Santa Clara CA) equipped with a C18 reversed-phase column (15 cm  $\times$  4.6 mm, 5  $\mu$ m) and UV detector (210 nm). The mobile phase was 50/50 (v/v) methanol/water at 1.0 mL/min. In the experiments with HA, 30/70 (v/v) acetonitrile/water was used as mobile phase to separate peaks of AN from HA. In the experiments with sediment porewater, samples were filtered using a 0.45  $\mu$ m syringe filter before HPLC analysis. Headspace  $H_2$  concentration was determined using GC/TCD as previously described.<sup>29</sup> Attempts to identify water-soluble oxidation products of AN were conducted using time-of-flight mass spectrometer following HPLC (HPLC-TOF-MS).

## RESULTS AND DISCUSSION

**Nitrobenzene Sequential Reduction/Oxidation.** Nitrobenzene can be completely removed by sequential reduction/oxidation with carbon felt electrodes. Figure 1 is an example of NB degradation at 3 V applied voltage. Nitrobenzene (NB,  $C_6H_5NO_2$ ) was stoichiometrically reduced to aniline (AN,  $C_6H_5NH_2$ ) via nitrosobenzene (NSB,  $C_6H_5NO$ ) by cathodic reactions in the electrolytic cell within 20 hours. Phenylhydroxylamin (PHA,  $C_6H_5NOH$ ), a short-lived intermediate<sup>30</sup>

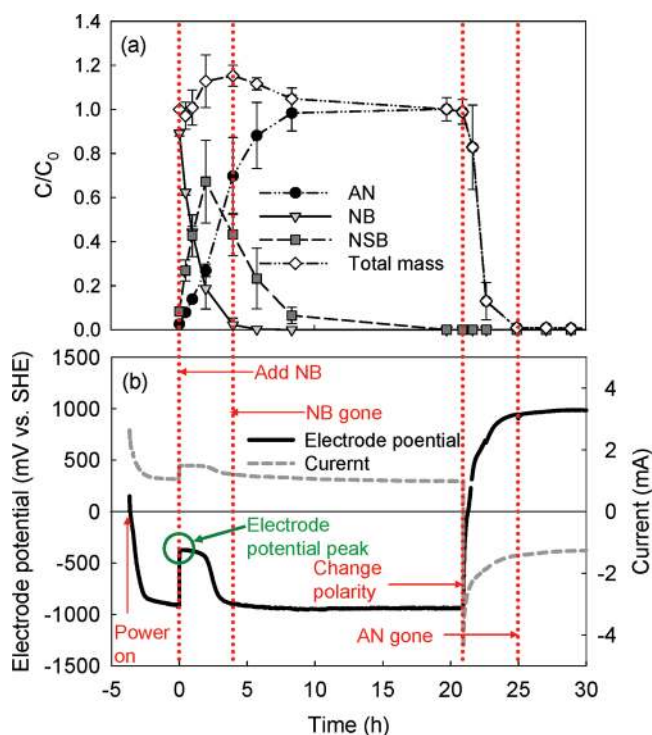


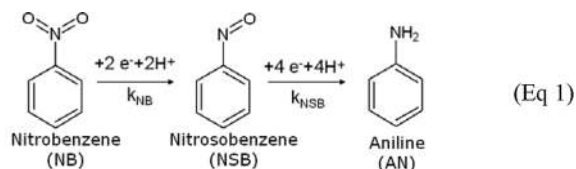
**Figure 1.** Sequential reduction/oxidation of nitrobenzene (NB) at 3 V applied voltage. (a) Relative molar concentrations of nitrobenzene (NB), nitrosobenzene (NSB), and aniline (AN) with regard to the initial (100  $\mu$ M) NB added. Error bars represent standard deviation of triplicate reactors. (b) Working electrode potential (vs SHE) and current as a function of time. The circle shows the electrode potential peak. NB was added into pure buffer solution (time zero) after the electrode potential had stabilized. After both NB and NSB were stoichiometrically converted to AN, the polarity of the electrodes were reversed.

of NSB reduction to AN, was not detected in this study. Following complete stoichiometric NB reduction to AN, the polarity of the working chamber was reversed and AN was rapidly removed under oxidizing conditions within 4 h. None of the commonly reported AN oxidation intermediates (catechol,<sup>20</sup> benzoquinone or maleic acid,<sup>19</sup> dianiline, 4-anilino phenol or azobenzol<sup>31</sup>) were detected by HPLC-TOF-MS. Polymerization products of AN<sup>32</sup> were not observed. pH in the working chamber was well buffered; at 3 V applied voltage, pH rose from 6.5 to 7 during reduction and decreased to 6.7 at the end of oxidation. Slow NB loss and no products were observed in the control reactor that was not powered (data not shown), indicating that sorption and alkaline hydrolysis were not significant removal mechanisms.

Inspection of Figure 1(b) shows that the working electrode potential is an indicator for reaction progression: prior to addition of NB, the only reaction occurring was water electrolysis and the electrode potential stabilized to a baseline ( $\sim -900$  mV vs SHE with an external potential of 3 V). The addition of NB (an oxidant) increased the electrode potential to  $-330$  mV, close the NB reduction potential ( $-356$  mV vs SHE) reported by Wang et al.<sup>33</sup> This potential immediately after NB addition is referred as “electrode potential peak” in Figure 1(b) and will be used in following discussion. The potential gradually decreased to its baseline as NB was completely reduced to AN. Reversing the polarity of the electrodes rapidly changed the electrode potential from cathodic to anodic. The potential continued to increase while AN was present and reached a steady value of  $\sim +1$  V once AN was completely removed. The potential profile, in conjunction with the concentration profiles with time is useful for analysis in the following sections.

The current data in Figure 1(b) follows a similar trend to the potential: current dropped and got stabilized at 1 mA after power on, and increased instantly to 1.5 mA after NB addition. After NB was totally reduced, current decreased back to 1 mA, and reversed its direction once the polarity was switched. Once AN was totally removed, current reached the steady level of 1 mA (but in opposite direction of flow).

AN oxidation is significantly faster than NB and NSB reduction (Figure 1), indicating that the reduction is rate-limiting for sequential reduction/oxidation of NB; therefore, the following degradation study focuses on reduction only. The nearly complete mass balance for NB reduction (Figure 1(a)) suggested that transformation of NB to AN via NSB can be modeled as two sequential first order reactions with observed rate constants  $k_{NB}$  (NB to NSB) and  $k_{NSB}$  (NSB to AN) as shown in eq 1:



The reduction stage of NB removal in Figure 1(a) was replotted in Figure 2 to fit the first order reaction kinetics. At 3 V, the NB and NSB reduction rate constant were 0.88  $h^{-1}$  and 0.36  $h^{-1}$ , respectively. The goodness of fit ( $R^2 > 0.99$ ) indicated that the sequential first order reactions were suitable to simulate the NB reduction kinetics.  $k_{NSB}$  determined independently from experiments using NSB as the parent compound was similar to

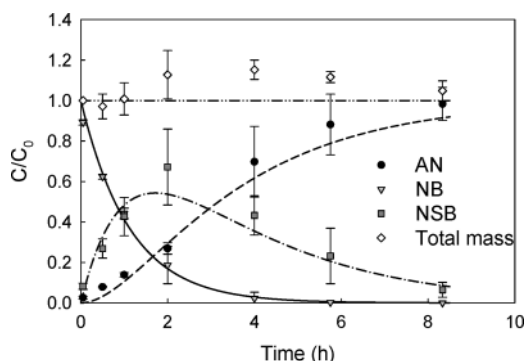


**Figure 2.** First order kinetic model fit for nitrobenzene (NB) reduction to aniline (AN) via nitrosobenzene (NSB) at 3 V. Symbols are observed concentration data and lines represent the model fit. Concentration data are the averages of triplicate reactors.

the rate constant extracted from experiments with NB as the parent compound (SI Figure S3).

**Effect of Voltage on Reduction Rate Constants.** For a reactive cap to mitigate contaminant transport into the overlying water, the contaminant degradation must be faster than the convection through the cap.<sup>34</sup> Since applied voltage is the thermodynamic driving force for the reaction, the observed decontamination rate should increase with increasing voltage, assuming the reaction kinetics is the rate-limiting step. The reduction rate constants of NB and NSB were found to be increased with applied voltage between 2 V ( $k_{\text{NB}} = 0.3 \text{ h}^{-1}$  and  $k_{\text{NSB}} = 0.04 \text{ h}^{-1}$ ) and 3.5 V ( $k_{\text{NB}} = 1.6 \text{ h}^{-1}$  and  $k_{\text{NSB}} = 0.64 \text{ h}^{-1}$ ) (Figure 3(a)). However, a higher voltage beyond 3.5 V did not cause greater  $k_{\text{NB}}$  or  $k_{\text{NSB}}$ , and below 2 V no reaction was observed. The voltage dependence of  $k_{\text{NB}}$  and  $k_{\text{NSB}}$  is consistent with the voltage dependence of the electrode potential peak when NB was added (illustrated in Figure 1(b)). The electrode potential peak (Figure 3b) decreased as voltage increased up to 3.5 V, but showed no difference between 3.5 and 4.5 V (the full profile of electrode potential over time under different applied voltage were presented in SI Figure S4(a)). Voltage in excess of 3.5 V was likely dissipated by ohmic losses in the electrolyte, rather than for cathodic reduction. Since electrode potential is the determining factor for reduction reaction to take place, the lack of a further decrease in the electrode potential peak with

increasing voltage prevented  $k_{\text{NB}}$  and  $k_{\text{NSB}}$  from further increase. pH, working electrode potential and current information for each experiment can be found in SI Table S1.

**Effect of Initial NB Concentration on Reduction Rate Constants.** The concentration of sediment contaminants is typically variable through the sediment and cap. Different initial NB concentrations were tested to determine if the observed reaction rate constants were dependent on initial contaminant concentration. Decreasing the initial NB concentration from 100 to 5  $\mu\text{M}$  increased the observed reduction rate constants by a factor of 9 for  $k_{\text{NB}}$  ( $0.88 \text{ h}^{-1}$  to  $7.9 \text{ h}^{-1}$ ) and 5 for  $k_{\text{NSB}}$  ( $0.36 \text{ h}^{-1}$  to  $1.7 \text{ h}^{-1}$ ) (Figure 4). Similar inverse correlation of initial

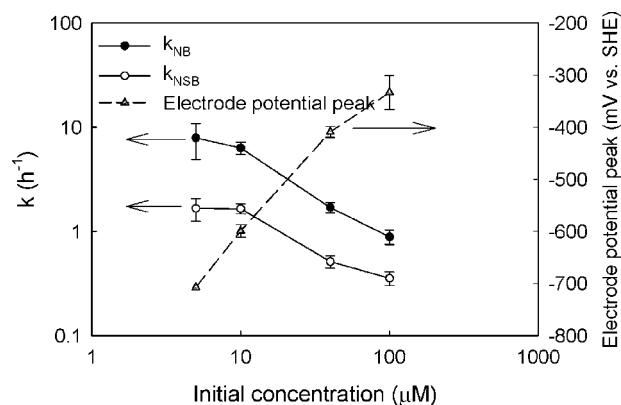


**Figure 4.** Effect of initial nitrobenzene concentration on nitrobenzene ( $k_{\text{NB}}$ ) and nitrosobenzene ( $k_{\text{NSB}}$ ) reduction rate constants, and on electrode potential peak after NB addition in the working chamber (electrode potential peak, as illustrated in Figure 1(b)) at 3 V. Results are averages of triplicate experiments. Error bars for reaction rate constants represent 95% confidence intervals for the modeled values, and for cathode potential peak represent the standard deviation of the triplicate reactors measured.

concentration with reduction rate constant of NB on an Fe(0) surface was attributed to competition for adsorption to a reactive iron surface.<sup>9</sup> In such a circumstance, the observed reduction rates are decided by both reaction kinetics and adsorption kinetics. Another interpretation is that, since NB is an oxidant, higher initial NB concentration lead to higher electrode potential peak (Figure 4). The higher (less negative)

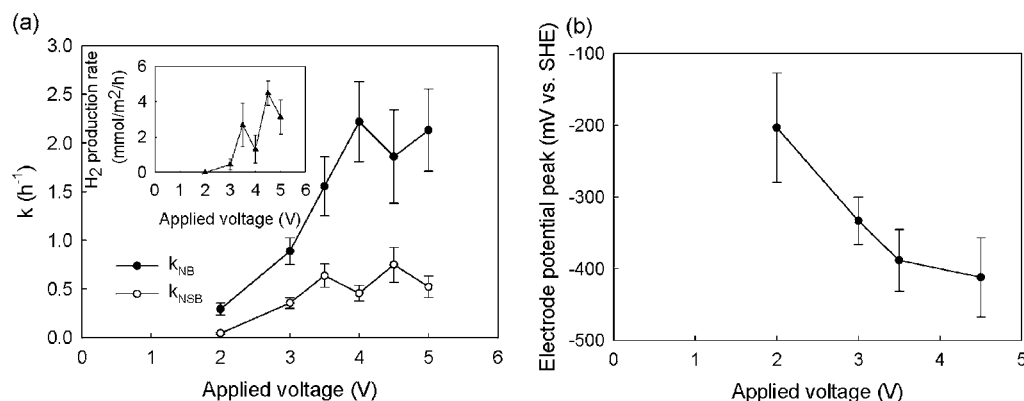


**Figure 3.** (a) Effect of applied voltage on the nitrobenzene ( $k_{\text{NB}}$ ) and nitrosobenzene ( $k_{\text{NSB}}$ ) reduction rate constants. Inset: Effect of applied voltage on the hydrogen production rate constant. (b) Electrode potential peak after NB addition in the working chamber (electrode potential peak, as illustrated in Figure 1(b)) under different applied voltages. Results are averages of triplicate reactors with 100  $\mu\text{M}$  initial nitrobenzene addition. Error bars in (a) represent the 95% confidence interval of the modeled rate constants, and in (b) represent the standard deviation of the triplicate reactors measured.

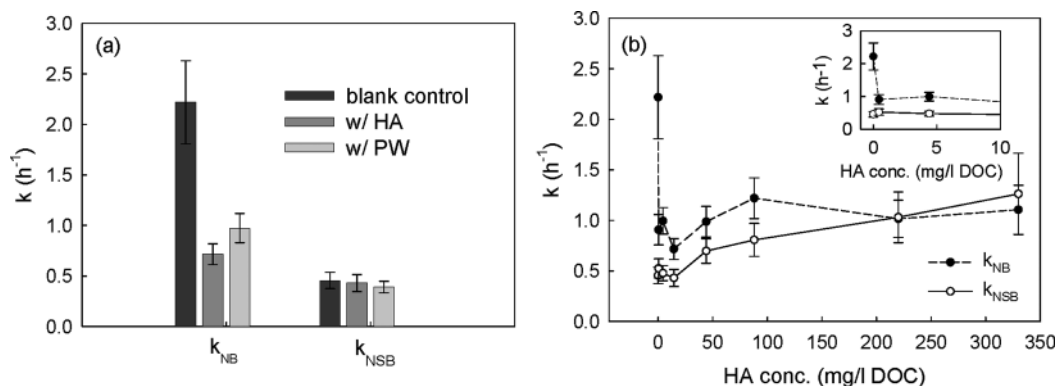


**Figure 5.** (a) Impact of NOM presence on nitrobenzene ( $k_{NB}$ ) and nitrosobenzene ( $k_{NSB}$ ) reduction rate constants. The chemical composition for each group was: blank control: 20 mM  $NaH_2PO_4$ ; w/HA: HA (14.4 mg/L DOC) and 20 mM  $NaH_2PO_4$ ; w/PW: simulated sediment porewater (14.4 mg/L DOC) and 20 mM  $NaH_2PO_4$ . (b) Impact of humic acid concentration on nitrobenzene ( $k_{NB}$ ) and nitrosobenzene ( $k_{NSB}$ ) reduction rate constants. The inset is the scale-up of low concentration data. For both figures, results are averages of triplicate experiments with 100  $\mu$ M initial nitrobenzene addition at 4 V, and error bars represent the 95% confidence interval of modeled rate constants.

electrode potential peak decreased the driving force for reaction and therefore slowed down the reaction.<sup>35</sup> The temporal variation of electrode potential for each initial NB concentration is available in SI Figure S4(b). pH, working electrode potential and current information for each experiment can be found in SI Table S1.

**Effect of NOM on Reduction Rate Constants.** The effect of NOM on NB reaction rate constants was examined using simulated sediment porewater (PW) or humic acid (HA) solution (both containing 14.4 mg/L DOC). Figure 5(a) indicates that  $k_{NB}$  decreases from 2.2  $h^{-1}$  in no NOM control to 0.7  $h^{-1}$  and 0.8  $h^{-1}$  in presence of porewater and HA solution, respectively; while in contrast,  $k_{NSB}$  was less affected, around 0.4  $h^{-1}$  in all the groups. Figure 5(a) also shows that HA solutions and simulated sediment porewaters with the same DOC concentrations have a similar effect on the NB and NSB reduction rate constants. This suggests that HA may be the key component in porewater responsible for the change of  $k_{NB}$  and  $k_{NSB}$ . Thus further study on the relationship between the NOM concentration and degradation rate was conducted with HA only. Figure 5(b) shows that very low concentrations of HA (0.44 mg/L DOC) decreased  $k_{NB}$  by 2 folds and the effect was not dependent on concentration of added HA over the range of typical DOC concentrations in sediment porewater (several mg/L to  $\sim$ 200 mg/L). This change of  $k_{NB}$  is within the range of 1.2–10-fold decrease in the reaction rate constant reported for HA effects on NB reduction by Fe(0).<sup>12</sup> In contrast,  $k_{NSB}$  slightly increased with HA concentration, as has been observed for NOM mediated NB chemical reduction by  $H_2S$ .<sup>10</sup> NOM did not likely affect the reduction rates by serving as an electron donor, since (1) no matter which source or what concentration of NOM was added, there was no statistically significant difference in electrode potential peak (data not shown) and (2) adding NOM to unpowered reactors could not cause NB reduction (data not shown). Potential explanations of the NOM effect on reduction rates are (a) NOM may competitively adsorb to the electrode surfaces (accumulation of HA on electrodes surfaces has been observed)<sup>12</sup> and increase the mass transfer resistance of NB or NSB from the bulk solution to the electrodes, thus decreased the reduction rate; or (b) NOM may increase the rate due to electron shuttling between the electrodes and contaminant. However, as Figure 5 shows, the impacts of NOM on  $k_{NB}$  and  $k_{NSB}$  were relatively small (less than a factor of 3) when compared to the impact of

applied voltage and initial contaminant concentration ( $\sim$ factor of 10), and therefore were not further investigated. pH, working electrode potential and current information for each experiment can be found in SI Table S1.

**Reaction Rate Comparison with Other Studies.** The NB reduction rate measured here was comparable to those previously reported using in microbial fuel cells (MFC),<sup>33,36</sup> however some differences are noteworthy. Wang et al.<sup>33</sup> used acetate oxidation instead of water oxidation (to  $O_2$ ) at the anode, so we compare reaction rates determined at the same cathode potential instead of at the same total applied voltage. In their study, when the applied voltage was 0.5 V, their cathode potential with preadded NB was  $-790$  mV (without bacteria) or  $-740$  mV (with bacteria). This is much lower than the cathode potential after NB addition at any applied voltage in this study (SI Figure S4). A lower cathode potential would be expected to lead to higher reaction rate. However,  $k_{NB}$  determined from their reported concentration vs time data at this cathode potential is only 0.045  $h^{-1}$  (without bacteria) and 0.2  $h^{-1}$  (with bacteria); while this study with an abiotic reaction only has a  $k_{NB}$  between 0.3 to 2.5  $h^{-1}$ . Although the cathode used in the study by Wang et al. was platinumized, the cathode surface area normalized reaction rate in their study ( $1.1 \times 10^{-3}$   $h^{-1}cm^{-2}$  without bacteria or  $1.0 \times 10^{-2}$   $h^{-1}cm^{-2}$  with bacteria) is slower than observed in the present study (between  $1.5 \times 10^{-2}$   $h^{-1}cm^{-2}$  and  $0.12$   $h^{-1}cm^{-2}$ ). Such comparison suggests that operating the electrodes at lower voltage may slow the desired degradation, but that the total power output can be greatly reduced (0.5 V for the study of Wang et al., vs at least 2 V in this study) using a suitable electron donor at the anode. It may be infeasible to continuously providing a suitable electron donor to a sediment cap but, in the cases of sequential reduction/oxidation, or removing contaminants mixtures requiring different redox conditions, pursuing such coupling is desirable.

Similarly, Li et al.<sup>36</sup> used microbial glucose oxidation at the anode to couple with NB reduction at cathode.  $k_{NB}$  determined from their reported concentration vs time data is  $\sim$ 0.8  $h^{-1}$  (or  $1.6 \times 10^{-2}$   $h^{-1}cm^{-2}$ ) for the initial 3 h and slowed down afterward. Such a reaction rate is close to the low end of the  $k_{NB}$  range obtained in this study. The cathode potential at such reaction rate was not reported, but since their cathode was not poised, it should be around the NB reduction potential found in both this study and the study by Wang et al.<sup>33</sup> Their current

density at such reaction rate was controlled constantly at 15 A/m<sup>3</sup> (or 165 mA/m<sup>2</sup>), while the maximum current density in this study was 125–375 mA/m<sup>2</sup>. Both the reaction and current density observed in this study were similar with these reported in Li's study.

**Performance and Design of Electrode-Based Reactive Cap.** We examined how the cap properties (thickness and reactivity) as well as contaminant transport properties (seepage velocity and diffusivity) affected the ability of an electrode-based reactive cap to degrade contaminants moving through by advection and diffusion. Since this model only considers terms which are relevant within a porous electrode, an electrophoretic term for the velocity was not considered. The case study of NB and the cap parameters used here are included as a metric for comparison to other important sediment contaminants that may have slower rates of reaction.

There are three steps during contaminant abiotic degradation at the electrode surfaces as studied here: diffusion of NB to the electrode surface, reaction of NB at the electrode surface, and diffusion of reaction products from the electrode surface. In the H-cell reactions, we assume that reaction at the electrode surface is the rate controlling step. This is reasonable since the time scale for diffusion in our system ( $t_{\text{diff}} = L^2/D$ ) is approximately 0.2s, assuming a diffusion layer thickness ( $L$ ) of 10  $\mu\text{m}$ <sup>37</sup> and NB diffusivity ( $D$ ) of  $4.4 \times 10^{-10}$  m<sup>2</sup>/s.<sup>37</sup> This is much shorter than the time scale for the first order reaction ( $t_{\text{rxn}} = 1/k$ , which is in minutes to hours for NB). Also the oxidation of AN is faster than reduction of NB and NSB (Figure 1). Thus the reduction reaction is rate limiting in the well mixed H-cell reactors. The reaction rate may also be assumed to be the rate-limiting step for other, more refractory contaminants with slower degradation kinetics, assuming the diffusivities are in the same magnitude.

In real sediment, within an electrode-based reactive cap, the overall decontamination rate is moderated by contaminant migration in surrounding medium. The steady state contaminant flux to each electrode can be simulated using a one-dimensional advection-diffusion-reaction model<sup>38</sup> with the analytical solution of

$$C(z) = C_0 \exp\left(\frac{v - \sqrt{v^2 + 4Dk}}{2D} z\right) \quad \text{When } 0 \leq z \leq h \quad (2)$$

Where  $z$  is the relative location of the interested point to the bottom of the electrode;  $C_0$  and  $C(z)$  are the contaminant concentrations in the porewater entering the cap and at position  $z$ , respectively;  $v$  is the upward sediment porewater average velocity;  $D$  is the diffusivity of contaminant;  $k$  is observed first order reaction rate constant;  $h$  is the electrode thickness.

To make the solution as general as possible, eq 4 can be rewritten in terms of the dimensionless Peclet Number ( $Pe$ ) and Damkohler number ( $Da$ ) that can be calculated for any sediment cap and contaminant.

$$Pe = \frac{vh}{D} = \frac{\text{advection rate}}{\text{diffusion rate}} \quad (3)$$

$$Da = \frac{kh}{v} = \frac{\text{reaction rate}}{\text{advection rate}} \quad (4)$$

Rewriting eq 4 in terms of  $Pe$  and  $Da$  allows assessment of contaminant removal efficiency ( $f$ ) for any cap or contaminant in general:

$$f = 1 - C(h)/C_0 = 1 - \exp\left(\frac{Pe - \sqrt{Pe^2 + 4DaPe}}{2}\right) \quad (5)$$

Figure 6 illustrates the fraction of contaminant removed vs the Peclet Number for a range of Damkohler numbers. Greater

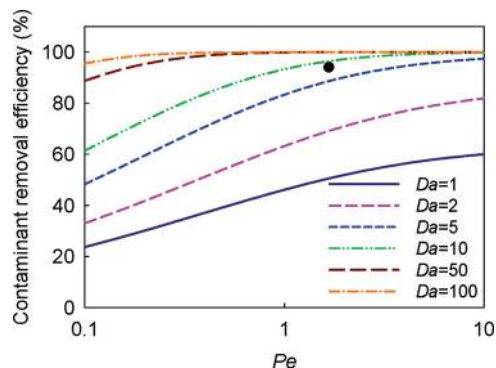


**Figure 6.** Effect of flow conditions (Peclet number,  $Pe$ ) on transformation in the sediment cap for a range of reactivity (Damkohler numbers,  $Da$ ). The single dot represents the electrode and NB reactivity data in this study ( $k = 0.5 \text{ h}^{-1}$ ,  $v = 1 \text{ cm/d}$ ,  $h = 0.635 \text{ cm}$ , and  $D = 4.4 \times 10^{-10} \text{ m}^2/\text{s}$ ).

than 80% removal can be achieved with electrode caps having  $Da > 5$  at  $Pe$  expected in sediment caps ( $Pe < 10$ , considering the typical sediment flow velocity of no more than a couple of cm/d, electrode thickness of a few cm, and effective diffusivity in the magnitude of  $10^{-10}$  m<sup>2</sup>/s). It is important to note that  $Pe$  and  $Da$  are not independent parameters, but rather covary with velocity, that is,  $Pe$  number decreases with decreasing porewater velocity, but  $Da$  increases with decreasing porewater velocity. Thus, for a given cap dimension, a lower  $Pe$  number usually accompanies a high  $Da$ . With the assumption of a typical porewater velocity of 1 cm/d, an electrode thickness of 0.635 cm (one layer of the graphite felt used in this study), a NB diffusivity of  $4.4 \times 10^{-10}$  m<sup>2</sup>/s,<sup>37</sup> and the reaction rate constant of  $0.5 \text{ h}^{-1}$  based on the reactivity data from this study, 94% NB degradation is predicted, shown as the single dot in Figure 6. Note diffusivity ( $D$ ) in water instead of effective diffusivity ( $D^*$ ) in the porous electrode is used due to lack data for electrode porosity ( $n$ ) and tortuosity ( $\tau$ ). Since  $D^* = Dn\tau$  and  $0 < n, \tau < 1$ ,  $D$  is always greater than  $D^*$ . Such an approximation therefore leads to underestimate of  $Pe$  and thus underestimate of removal efficiency.

Other contaminants may not be as easily degraded as NB, and considering that the reaction rate increase with applied voltage are not unlimited, a specific removal efficiency for a particular contaminant may require a degradation rate beyond what the electrode-based reactive cap can provide. In this case, a thicker cap is needed to provide longer hydraulic retention times for the completion of the desired reactions. In addition, though a particular reaction rate may be achievable with a high applied voltage, in many cases it may be desirable to operate at a lower voltage. In this case electrode thickness may be increased to provide the desired removal efficiency. Operating at low voltage can decrease energy costs and environmental

disturbance (e.g., pH change). This is especially true for operation at a voltage which transforms contaminants without hydrogen production (e.g., in Figure 3(a), at 2 V NB and NSB were reduced without hydrogen production). Electrode-based sediments caps will need to be optimized for both design (electrode thickness) and operational (applied voltage) conditions to minimize remediation costs.

It is worth noting that in real sediments mass transfer processes and reactions other than those considered here may also affect the contaminant degradation rates. For example, unlike the NB probe in this study, highly hydrophobic contaminants may strongly adsorb to sediment NOM. Slow desorption from NOM may result in a low contaminant transport rate to the electrode surface, and thus a lower overall removal rate. Also, no electrokinetic term is incorporated in this model, because this model only discusses contaminants behaviors inside the electrode. By ignoring the potential gradient in the porewater inside the electrode, electric potential is considered equal at all positions within the electrode, and electromigration and electroosmosis driven by electric potential gradient become zero. A more complicated model dealing with the heterogeneous potential distribution may be needed for advanced analysis. Other reactions may also need to be considered for the cap design. For instance, hydrogen produced at the cathode (Figure 3(a) inset) may be utilized by bacteria for contaminant biodegradation. The participation of microbial activity may increase the reactivity ( $Da$ ) over that of the electrode alone.<sup>33</sup> This is potentially the case for contaminants (such as PCBs) with low abiotic reduction rates, as long as the supplementary biological reduction rate in the presence of low levels of  $H_2$  is high enough to make the electrode-based reactive cap feasible. Either of these conditions would require incorporating mass transfer into the model, or the in situ reaction rates, to optimize the design of the cap.

## ■ ASSOCIATED CONTENT

### 📄 Supporting Information

(1) Conceptual model for the electrode-based reactive sediment cap; (2) Schematic overview of the H-cell reactors employed in this work; (3) comparison of NSB reduction rate constant ( $k_{NSB}$ ) simultaneously fitted from NB reduction and  $k_{NSB}$  fitted directly from NSB reduction; (4) cathode potential vs time during NB reduction at different applied voltage and different initial NB concentration; (5) pH, working electrode potential and current information for each experiment. This material is available free of charge via the Internet at <http://pubs.acs.org>.

## ■ AUTHOR INFORMATION

### Corresponding Author

\*Phone: 412-268-9811; fax: 412-268-7813; e-mail: kelvin@cmu.edu.

### Notes

The authors declare no competing financial interest.

## ■ ACKNOWLEDGMENTS

We thank Palwinder Kaur (US Department of Energy, National Energy Technology Laboratory, Pittsburgh, PA) for assisting mass spectrometer analysis. The project described was supported by Award No.: 1R01 ES016154-01 from the National Institute of Environmental Health Sciences, National Institute of Health. The content is solely the responsibility of

the authors and does not necessarily represent the official views of the NIEHS or the NIH.

## ■ REFERENCES

- (1) Palermo, M.; Maynard, S.; Miller, J.; Reible, D., Guidance for in situ subaqueous capping of contaminated sediments. In Great Lakes National Program Office: Chicago, 1998.
- (2) McDonough, K. M.; Murphy, P.; Olsta, J.; Zhu, Y. W.; Reible, D.; Lowry, G. V. Development and placement of a sorbent-amended thin layer sediment cap in the Anacostia River. *Soil Sed. Contam.* **2007**, *16* (3), 313–322.
- (3) Jacobs, P. H.; Forstner, U. Concept of subaqueous capping of contaminated sediments with active barrier systems (ABS) using natural and modified zeolites. *Water Res.* **1999**, *33* (9), 2083–2087.
- (4) Choi, H.; Agarwal, S.; Al-Abed, S. R. Adsorption and Simultaneous Dechlorination of PCBs on GAC/Fe/Pd: Mechanistic aspects and reactive capping barrier concept. *Environ. Sci. Technol.* **2009**, *43* (2), 488–493.
- (5) Sun, H.; Xu, X.; Gao, G.; Zhang, Z.; Yin, P. A novel integrated active capping technique for the remediation of nitrobenzene-contaminated sediment. *J. Hazard. Mater.* **2010**, *182* (1–3), 184–190.
- (6) Sun, M.; Yan, F.; Zhang, R.; Reible, D. D.; Lowry, G. V.; Gregory, K. B. Redox control and hydrogen production in sediment caps using carbon cloth electrodes. *Environ. Sci. Technol.* **2010**, *44* (21), 8209–8215.
- (7) Aulenta, F.; Tocca, L.; Verdini, R.; Reale, P.; Majone, M. Dechlorination of trichloroethene in a continuous-flow bioelectrochemical reactor: Effect of cathode potential on rate, selectivity, and electron transfer mechanisms. *Environ. Sci. Technol.* **2011**, *45* (19), 8444–8451.
- (8) Tsyganok, A. I.; Otsuka, K. Selective dechlorination of chlorinated phenoxy herbicides in aqueous medium by electrocatalytic reduction over palladium-loaded carbon felt. *Appl. Catal., B* **1999**, *22* (1), 15–26.
- (9) Arnold, W. A.; Roberts, A. L. Pathways and kinetics of chlorinated ethylene and chlorinated acetylene reaction with Fe(0) particles. *Environ. Sci. Technol.* **2000**, *34* (9), 1794–1805.
- (10) Dunnivant, F. M.; Schwarzenbach, R. P.; Macalady, D. L. Reduction of substituted nitrobenzenes in aqueous solutions containing natural organic matter. *Environ. Sci. Technol.* **1992**, *26* (11), 2133–2141.
- (11) Eriksson, J.; Frankki, S.; Shchukarev, A.; Skyllberg, U. Binding of 2,4,6-trinitrotoluene, aniline, and nitrobenzene to dissolved and particulate soil organic matter. *Environ. Sci. Technol.* **2004**, *38* (11), 3074–3080.
- (12) Keum, Y.-S.; Li, Q. X. Reduction of nitroaromatic pesticides with zero-valent iron. *Chemosphere* **2004**, *54* (3), 255–263.
- (13) Chiou, C. T.; Kile, D. E.; Brinton, T. I.; Malcolm, R. L.; Leenheer, J. A.; MacCarthy, P. A comparison of water solubility enhancements of organic solutes by aquatic humic materials and commercial humic acids. *Environ. Sci. Technol.* **1987**, *21* (12), 1231–1234.
- (14) Kilduff, J. E.; Karanfil, T.; Weber, W. J. Competitive interactions among components of humic acids in granular activated carbon adsorption systems: Effects of solution chemistry. *Environ. Sci. Technol.* **1996**, *30* (4), 1344–1351.
- (15) Lohner, S. T.; Becker, D.; Mangold, K.-M.; Tiehm, A. Sequential reductive and oxidative biodegradation of chloroethenes stimulated in a coupled bioelectro-process. *Environ. Sci. Technol.* **2011**, *45* (15), 6491–6497.
- (16) Preuss, A.; P. G. Rieger, Anaerobic transformation of 2,4,6-trinitrotoluene. In *Biodegradation of Nitroaromatic Compounds*; Spain, J. C., Ed.; Plenum Press: New York, 1995.
- (17) Rieger, P. G.; H. J. Knachmuss, Basic knowledge and perspectives on biodegradation of 2,4,6-trinitrotoluene and related nitroaromatic compounds in soil. In *Biodegradation of Nitroaromatic Compounds*; Spain, J. C., Ed.; Plenum Press: New York, 1995.

(18) Nishino, S. F.; Spain, J. C. Degradation of nitrobenzene by a *Pseudomonas pseudoalcaligenes*. *Appl. Environ. Microbiol.* **1993**, *59* (8), 2520–2525.

(19) Kirk, D. W.; Sharifian, H.; Foulkes, F. R. Anodic oxidation of aniline for waste water treatment. *J. Appl. Electrochem.* **1985**, *15* (2), 285–292.

(20) Lyons, C. D.; Katz, S.; Bartha, R. Mechanisms and pathways of aniline elimination from aquatic environments. *Appl. Environ. Microbiol.* **1984**, *48* (3), 491–496.

(21) Mu, Y.; Rozendal, R. A.; Rabaey, K.; Keller, J. Nitrobenzene removal in bioelectrochemical systems. *Environ. Sci. Technol.* **2009**, *43* (22), 8690–8695.

(22) Dickel, O.; Haug, W.; Knackmuss, H.-J. Biodegradation of nitrobenzene by a sequential anaerobic-aerobic process. *Biodegradation* **1993**, *4* (3), 187–194.

(23) Gilbert, D. M.; Sale, T. C. Sequential electrolytic oxidation and reduction of aqueous phase energetic compounds. *Environ. Sci. Technol.* **2005**, *39* (23), 9270–9277.

(24) Wani, A. H.; O'Neal, B. R.; Gilbert, D. M.; Gent, D. B.; Davis, J. L. Electrolytic transformation of ordinance related compounds (ORCs) in groundwater: Laboratory mass balance studies. *Chemosphere* **2006**, *62* (5), 689–698.

(25) Gregory, K. B.; Lovley, D. R. Remediation and recovery of uranium from contaminated subsurface environments with electrodes. *Environ. Sci. Technol.* **2005**, *39* (22), 8943–8947.

(26) Reimers, C. E.; Tender, L. M.; Fertig, S.; Wang, W. Harvesting energy from the marine sediment-water interface. *Environ. Sci. Technol.* **2001**, *35* (1), 192–195.

(27) Tender, L. M.; Reimers, C. E.; Stecher, H. A.; Holmes, D. E.; Bond, D. R.; Lowy, D. A.; Pilobello, K.; Fertig, S. J.; Lovley, D. R. Harnessing microbially generated power on the seafloor. *Nat. Biotechnol.* **2002**, *20* (8), 821–825.

(28) Rezaei, F.; Richard, T. L.; Brennan, R. A.; Logan, B. E. Substrate-enhanced microbial fuel cells for improved remote power generation from sediment-based systems. *Environ. Sci. Technol.* **2007**, *41* (11), 4053–4058.

(29) Liu, Y.; Majetich, S. A.; Tilton, R. D.; Sholl, D. S.; Lowry, G. V. TCE dechlorination rates, pathways, and efficiency of nanoscale iron particles with different properties. *Environ. Sci. Technol.* **2005**, *39* (5), 1338–1345.

(30) Sternson, L. A.; DeWitte, W. J. High-pressure liquid chromatographic analysis of aniline and its metabolites. *J. Chromatogr.* **1977**, *137* (2), 305–314.

(31) Li, Y.; Wang, F.; Zhou, G.; Ni, Y. Aniline degradation by electrocatalytic oxidation. *Chemosphere* **2003**, *53* (10), 1229–1234.

(32) Matsushita, M.; Kuramitz, H.; Tanaka, S. Electrochemical oxidation for low concentration of aniline in neutral pH medium: application to the removal of aniline based on the electrochemical polymerization on a carbon fiber. *Environ. Sci. Technol.* **2005**, *39* (10), 3805–3810.

(33) Wang, A.-J.; Cheng, H.-Y.; Liang, B.; Ren, N.-Q.; Cui, D.; Lin, N.; Kim, B. H.; Rabaey, K. Efficient reduction of nitrobenzene to aniline with a biocatalyzed cathode. *Environ. Sci. Technol.* **2011**, *45* (23), 10186–10193.

(34) Murphy, P.; Marquette, A.; Reible, D.; Lowry, G. V. Predicting the performance of activated carbon-, coke-, and soil-amended thin layer sediment caps. *J. Environ. Eng.* **2006**, *132* (7), 787–794.

(35) Newman, J.; Thomas-Alyea, K. E. *Electrochemical systems*, 3rd ed.; Wiley-Interscience: New York, 2004; pp 203–240.

(36) Li, J.; Liu, G.; Zhang, R.; Luo, Y.; Zhang, C.; Li, M. Electricity generation by two types of microbial fuel cells using nitrobenzene as the anodic or cathodic reactants. *Bioresour. Technol.* **2010**, *101* (11), 4013–4020.

(37) Smeltzer, J. C.; Fedkiw, P. S. Reduction of nitrobenzene in a parallel-plate reactor. *J. Electrochem. Soc.* **1992**, *139* (5), 1358–1366.

(38) Schwarzenbach, R. P.; Gschwend, P. M.; Imboden, D. M., *Environmental Organic Chemistry*, 2nd ed.; Wiley-Interscience: 2002; pp 1006–1009.